Theoretical Investigation of α-decay Chains of Fm-Isotopes

Joshua T. Majekodunmi[1], N. Jain[2], Shilpa Rana[2*], K. Anwar[1], N. Abdullah[1] M. Bhuyan[3], and Raj Kumar[2]

[1]*Institute of Engineering Mathematics, Faculty of Applied and Human Sciences, Universiti Malaysia Perlis, Arau, 02600, Perlis, Malaysia*

[2]*School of Physics and Materials Science, Thapar Institute of Engineering and Technology, Patiala, Punjab 147004, India*

[3]*Center for Theoretical and Computational Physics, Department of Physics, Faculty of Science, University of Malaya, Kuala Lumpur 50603, Malaysia*

*srana60_phd19@thapar.edu (Corresponding Author)

ABSTRACT

Background: The theoretical and experimental investigations of decay properties of heavy and superheavy nuclei are crucial to explore the nuclear structure and reaction dynamics.

Purpose: The aim of this study is to probe the α-decay properties of ^{243}Fm and ^{245}Fm isotopic chains using the relativistic mean-field (RMF) approach within the framework of the preformed cluster-decay model (PCM).

Methods: The RMF densities are folded with the relativistic R3Y NN potential to deduce the nuclear interaction potential between the α particle and daughter nucleus. The penetration probability is calculated within the WKB approximation.

Results: The α-decay half-lives of even-odd ^{243}Fm and ^{245}Fm isotopes and their daughter nuclei are obtained from the preformed cluster-decay model. These theoretically calculated half-lives are found to be in good agreement with the recent experimental measurements.

Conclusions: The novel result here is the applicability of the scaling factor within the PCM as a signature for shell/sub-shell closures in α-decay studies. We have also demonstrated that N=137, 139 and Z=94 corresponding to ^{231,233}Pu could be shell/sub-shell closures. The least $T_{1/2}$ is found at ^{243,245}Fm which indicate their individual stability and α-decay as their most probable decay mode.

1. Introduction

Alpha decay is the most prominent mode of decay in the heavy and superheavy nuclei (SHN). Gamow [1], Gurney and Condon [2] independently provided the first theoretical explanation of the alpha decay process through the Quantum tunneling phenomenon. Since then, myriad of experimental as well as theoretical efforts have been devoted to probe the alpha decay properties of various nuclei [3-9]. The study of alpha decay provides insightful information about the nuclear structure, shell closure and fusion-fission dynamics [3-9]. The detection of alpha decay chains from an unknown nucleus followed by spontaneous fission provides an efficient tool to identify the synthesis of new elements in superheavy region [6-9]. Moreover, the exploration of alpha decay properties of actinides also plays an important role in materials science [10].

Numerous theoretical models such as the generalized liquid drop model (GLDM), multi-channel cluster model (MCCM) and density dependent cluster model (DDCM) etc. have been developed to probe the α-cluster radioactivity [11-14]. Generally, the alpha particle is perceived to pre-exist within the parent nucleus before its emission [15-17]. The quantum mechanical fragmentation theory (QMFT) based preformed cluster-decay model (PCM) also reinforces the theory of α-preformation [18-20]. In the PCM, an α-cluster is supposed to be preborn inside the parent nucleus which afterwards penetrates the interaction barrier formed due to the interplay between the attractive nuclear potential and repulsive Coulomb potential [18-20]. The deduction of Coulomb potential formed between the daughter nuclei and α-particle is straightforward unlike the nuclear potential. Various phenomenological, semi-microscopic and microscopic models have been adopted for the estimation of nuclear potential [20] and references therein.

The double folding approach [21] equipped with relativistic mean-field (RMF) densities and microscopic R3Y nucleon-nucleon (NN) potential have also been

applied lately to explore various nuclear phenomenon such as the nuclear radioactivity and nuclear fusion [22-25]. In a recent experiment [26], the α-decay half lives of two Fm-isotopes namely, ^{243,245}Fm and their respective daughter nuclei were measured. The authors demonstrated the detection of the previously unknown ^{235}Cm in the α-decay chain of ^{243}Fm isotope. This spurs us to theoretically investigate the decay properties of ^{243,245}Fm within PCM furnished with microscopic RMF formalism. The well-adopted Wentzel–Kramers–Brillouin (WKB) approximation is used to deduce the emission probability of the α-particle within the framework of PCM [18-20]. The preformation probability is calculated using the analytic formula proposed by Deng and Zhang [27-28]. The nuclear densities and R3Y NN potential obtained for non-linear NL3* RMF parameter set are folded to obtain the nuclear potential. The paper is structured as follows: the brief discussion of the RMF formalism and PCM is given in Sec 2. The results obtained from the theoretical calculations are discussed in Sec. 3. Lastly, the summary and important conclusion drawn from this study are given in Sec. 4.

2. Theoretical Formalism

The nucleus is considered to be a composite system of nucleons interacting via the exchange of mesons and photons in the relativistic mean field (RMF) theory [29-32]. The non-linear RMF relativistic Lagrangian density used to describe the interaction between nucleons through mesons and photons [22-25, 29-32] is expressed as

$$
\begin{aligned}
\mathcal{L} = &\bar{\psi}\left\{i\gamma^{\mu}\partial_{\mu} - M\right\}\psi + \frac{1}{2}\partial^{\mu}\sigma\partial_{\mu}\sigma - \frac{1}{2}m_{\sigma}^{2}\sigma^{2} - \frac{1}{3}g_{2}\sigma^{3} \\
&- \frac{1}{4}g_{3}\sigma^{4} - g_{\sigma}\bar{\psi}\psi\sigma - \frac{1}{4}\Omega^{\mu\nu}\Omega_{\mu\nu} + \frac{1}{2}m_{\omega}^{2}\omega^{\mu}\omega_{\mu} - g_{\omega}\bar{\psi}\gamma^{\mu}\psi\omega_{\mu} \\
&- \frac{1}{4}\vec{B}^{\mu\nu}\cdot\vec{B}_{\mu\nu} + \frac{1}{2}m_{\rho}^{2}\vec{\rho}^{\mu}\cdot\vec{\rho}_{\mu} - g_{\rho}\bar{\psi}\gamma^{\mu}\vec{\tau}\psi\cdot\vec{\rho}^{\mu} - \frac{1}{4}F^{\mu\nu}F_{\mu\nu} \\
&- e\bar{\psi}\gamma^{\mu}\frac{(1-\tau_{3})}{2}\psi A_{\mu}.
\end{aligned}
\tag{1}
$$

Here, all the symbols retain their usual meanings as can be found in [22-23] and reference therein. The effective R3Y NN interaction deduced from RMF equations of motion [22-25] including the single nucleon exchange effect is expressed as

$$
\begin{aligned}
V_{eff}^{R3Y}(r) = &\frac{g_{\omega}^{2}}{4\pi}\frac{e^{-m_{\omega}r}}{r} + \frac{g_{\rho}^{2}}{4\pi}\frac{e^{-m_{\rho}r}}{r} - \frac{g_{\sigma}^{2}}{4\pi}\frac{e^{-m_{\sigma}r}}{r} \\
&+ \frac{g_{2}^{2}}{4\pi}r\,e^{-2m_{\sigma}r} + \frac{g_{3}^{2}}{4\pi}\frac{e^{-3m_{\sigma}r}}{r} + J_{00}(E)\delta(r).
\end{aligned}
\tag{2}
$$

The nuclear interaction potential $V_{n}(R)$ between the emitted α-cluster and daughter nucleus is calculated by integrating this R3Y NN potential over nuclear densities within the well-known double folding approach [21] as

$$
V_{n}(\vec{R}) = \int \rho_{\alpha}(\vec{r}_{\alpha})\rho_{d}(\vec{r}_{d})V_{eff}\left(\left|\vec{r}_{\alpha} - \vec{r}_{d} + \vec{R}\right| \equiv r\right)d^{3}r_{\alpha}d^{3}r_{d}. \tag{3}
$$

Here, the densities of emitted α-clusters and daughter nuclei (d) are represented by ρ_{α} and ρ_{d} respectively. This nuclear potential along with the Coulomb potential are used to calculate decay half-lives within the Preformed Cluster-Decay Model (PCM) [18-19]. In the PCM, the decay constant and half-life $T_{1/2}$ for alpha decay are given as

$$
\lambda = \nu_{0}P_{\alpha}P, \ T_{1/2} = \frac{\ln 2}{\lambda}. \tag{4}
$$

Here, P is the penetration probability and is written as,

$$
P = P_{i}P_{b}. \tag{5}
$$

P_{i} and P_{b} are the penetration probabilities from R_{a} to a de-excitation point R_{i} and from R_{i} to R_{b}, respectively. The de-excitation probability (W_{i}) at R_{i} is taken as one. P_{i} and P_{b} are deduced within the well-adopted WKB approximation [18-20] as,

$$
P_{i} = \exp\left[-\frac{2}{h}\int_{R_{a}}^{R_{i}}\left\{2\mu\left[V(R) - V(R_{i})\right]\right\}^{1/2}dR\right], \tag{6}
$$

and

$$
P_{b} = \exp\left[-\frac{2}{h}\int_{R_{i}}^{R_{b}}\left\{2\mu\left[V(R_{i}) - Q\right]\right\}^{1/2}dR\right]. \tag{7}
$$

Here μ is the reduced mass given by $\mu = A_{d}A_{\alpha}/(A_{d} + A_{\alpha})$. The above integrals in Eqs. (6) and (7) are solved analytically [33]. The preformation probability P_{α} is calculated from the analytic formula of Deng and Zhang [27-28] and given as:

$$
\begin{aligned}
\log_{10} P_{\alpha} = &a + bA^{1/6}\sqrt{Z} \\
&+ c\frac{z}{\sqrt{Q_{\alpha}}} - \kappa\chi' - e\rho' + f\sqrt{l(l+1)},
\end{aligned}
\tag{8}
$$

where

$$
\chi' = Z_{\alpha}Z_{d}\sqrt{\frac{A_{\alpha}A_{d}}{(A_{\alpha} + A_{d})Q_{\alpha}}}
$$

$$
\rho' = \sqrt{\frac{A_{\alpha}A_{d}}{(A_{\alpha} + A_{d})}}Z_{\alpha}Z_{d}\left(A_{\alpha}^{1/3} + A_{d}^{1/3}\right).
$$

This formula accurately predicts the α-decay half-lives for known as well as unknown SHN. Here A and Z represent the mass and proton number of the decaying parent nucleus. Angular momentum carried by α-particle is denoted by $\ell=0$. The adjustable parameters a, b, c, e, f, and k were fitted to the experimental data as mentioned in Ref. [27], and

their respective values are the same for the $N \leq 126$ region as given in Ref. [28].

3. Results and Discussion

This section explains the results obtained for the ground state decay properties of even-odd Fermium isotopic chains. The ground state decay properties along the isotopic chains of even-odd ^{243}Fm and ^{245}Fm nuclei are investigated using the WKB approximation within the preformed cluster-decay model (PCM) as illustrated in the preceding section. Eq. (8) is employed to estimate the preformation probabilities P_α. The nuclear interaction potential is calculated by folding the relativistic mean-field (RMF) based R3Y NN potential for the NL3* parameter set with the respective densities of alpha and daughter nuclei. The effective interaction potential in Fig. 1 illustrates the cluster penetration process across the potential barrier. This involves the initial penetration from

the 1st classical turning point R_a to a point R_i where de-excitation (W_i) sets in. This is immediately accompanied by the penetration from point R_i to R_b whose potential $V(R_b)$ corresponds to the Q_α-value. The decay energies (Q_α) are taken from Ref. [26]. The only adjustable parameter within the PCM is the neck-length ΔR, which encapsulates the neck-formation and deformation effect as fragment separates during the decay process. Hence, ΔR determines the 1st turning point of the barrier penetration and can be optimized for each decay channel in order to predict their corresponding experimental half-life $T_{1/2}^{Expt}$. Elaborate details about the range of proximity of ΔR can be found in Refs. [34, 35] and the references therein. Other decay properties such as the barrier lowering (ΔV_B), driving potential $V(R_a)$-Q, penetrability (P) and decay constant (λ) are analysed for each reaction system in the first decay chain (^{243}Fm $\rightarrow$ ^{239}Cf $\rightarrow$ ^{235}Cm) and the second decay chain (^{245}Fm $\rightarrow$ ^{241}Cf $\rightarrow$ ^{237}Cm) are displayed in Table 1.

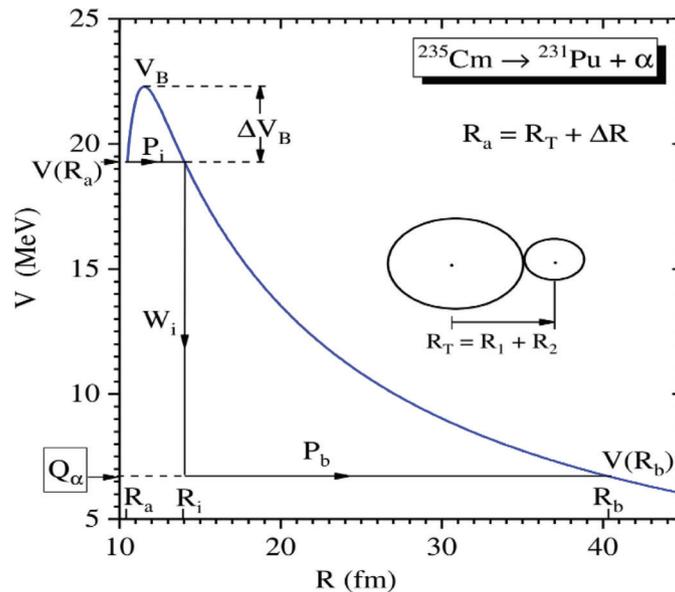**Figure 1:** The effective nuclear interaction potential (Eq. (3)) using the R3Y(NL3*) NN potential as a representative case of ^{235}Cm $\rightarrow$ ^{231}Pu+α.

Table1: Theoretical predictions of the α-decay properties of ^{243,245}Fm decay chains using the R3Y(NL3*) parameter set. The Q_α values and $T_{1/2}^{Expt}$ are taken from the recent experimental measurement of Khuyagbaatar et al.[26].

Parent Nuclei	Decay Channel	ΔR (fm)	Scaling Factor	ΔV_B (MeV)	$V(R_a)$-Q_α(MeV)	Q_α(MeV)	P_0	P	λ (s^{-1})	$T_{1/2}$ (s)	$T_{1/2}^{Expt}$ (s)
^{243}Fm	^{239}Cf+^{4}He	1.876	10^{-04}	-0.877	13.675	8.546	0.044	2.48×10^{-16}	68.500	0.231	0.231(9)
^{239}Cf	^{235}Cm+^{4}He	1.818	10^{-04}	-1.046	14.051	7.636	0.063	1.48×10^{-18}	0.389	28.060	28(2)
^{235}Cm	^{231}Pu+^{4}He	1.488	10^{-03a}	-2.97	12.632	6.690	0.099	9.45×10^{-21}	0.023	299.897	300
^{245}Fm	^{241}Cf+^{4}He	1.903	10^{-04}	-0.683	14.271	8.155	0.047	1.30×10^{-17}	3.500	4.200	4.20
^{241}Cf	^{237}Cm+^{4}He	1.721	10^{-04}	-1.662	13.572	7.342	0.068	2.83×10^{-19}	0.073	141.200	141
^{237}Cm	^{233}Pu+^{4}He	1.510	10^{-03a}	-2.493	13.175	6.656	0.098	4.36×10^{-21}	0.011	663.160	>600

^{a}This enhanced scaling factor indicates the presence of a sub-shell closure at ^{231,233}Pu.

It is worth noting that both the parent nuclei and the decay fragments are considered to be in the ground state in the present work. This implies that within this PCM framework, the temperature effect is ruled-out *i.e.* ($T = 0$). Despite, it has been demonstrated that with such assumption, the calculation of $T_{1/2}$ requires a constant scaling factor of 10^{-04} [36-37]. This earlier assertion is confirmed in column 4 of Table 1 for the participating reaction systems. However, the decay channels ^{231}Pu+^{4}He and ^{233}Pu+^{4}He displays a departure from the norm (highlighted in the footnote a), signifying the presence of a shell/sub-shell closure at *N=139, 141* and *Z=94* which corresponds to ^{231}Pu and ^{233}Pu, respectively. This is somewhat reminiscent of the appearance of peaks/kinks in symmetry energy of finite nuclei across the isotopic chain as indicators of shell/sub-shell closures [38-40]. In this regard, we have shown that the scaling factor within the PCM provides an easy avenue for the prediction of sub-shell closures in α-decay studies.

It is apparent that *ΔR* monotonously decreases down the decay chains. Specifically, the adjustable neck-length of first decay chain is bounded within the range (1.876-1.488)fm while the second lies between (1.903-1.510)fm as shown in in column 3 of Table 1. As such both scenarios exhibit similar behavior. A careful inspection of the difference between the neck-length of each successive reaction shows that *ΔR* could be relatively lower for daughter nuclei ^{231}Pu and ^{233}Pu. Further, the neck-length parameter modifies the entrance channel and incorporates the barrier lowering effect (whose associated parameter is denoted as *ΔV$_{B}$*) via the maximum barrier height V_{B} and the potential at the first classical turning point $V(R_{a})$.

The barrier lowering parameter ($ΔV_{B} = V(R_{a})-V_{B}$) in each case is recorded in the 5thcolumn of Table 1. Here, *ΔV$_{B}$* is found to decline with each successive decay. However, the driving potential $V(R_{a})$- $Q_{α}$ is equally influenced by the energy available for the decay process ($Q_{α}$-value) and the

potential $V(R_{a})$. The variations directly portray the barrier characteristics of the respective systems. Besides, the $Q_{α}$ values in column 7 are taken from the recent experimental data of Ref. [26] to ensure an accurate prediction of the observables. It should be noted that a positive Q-value is necessary for the reaction/decay process.

The inter-relationship between the $Q_{α}$-values as well as the preformation probability $P_{α}$ and penetration probability P is quite obvious from columns 7-9 of the Table 1. In essence, the $Q_{α}$-value is directly proportional to the P but exhibit an inverse relationship with the $P_{α}$. This implies that α-particle penetration decreases with decreasing $Q_{α}$-value while the same process hastens the preformation of α-particle within the parent nuclei. A very interesting phenomenon can be deduced as one compares the decay constants λ and their corresponding half-life $T_{1/2}$ predictions. Notably, these two observables are inversely proportional to each other and gives ample information about the stability of their respective parent nucleus. As presented in column 11 of Table 1 and Fig. 2, the least predicted half-life (largest λ) in each chain is found at ^{243}Fm and ^{245}Fm, having a relatively stabilized shell. This suggests that α-decay is the most probable decay mode of the mentioned nuclei. The reverse is noticed for ^{235}Cm and ^{237}Cm nuclei. Withal, the calculated half-lives are consistent with the recently measured half-lives [10]. From both graphs in the figure, it is obvious that $log_{10} T_{1/2}$ increases with increase in the neutron number of each nuclei and vice versa. It is imperative to note that for ^{237}Cm $\rightarrow$ ^{233}Pu+^{4}He, only the experimental lower limit is known at present. Beside the fact that our result is in perfect conformity with this observed limit, the calculated $T_{1/2} = 663.16$s is suggested (for further experimental test) as the precise half-life for this reaction.
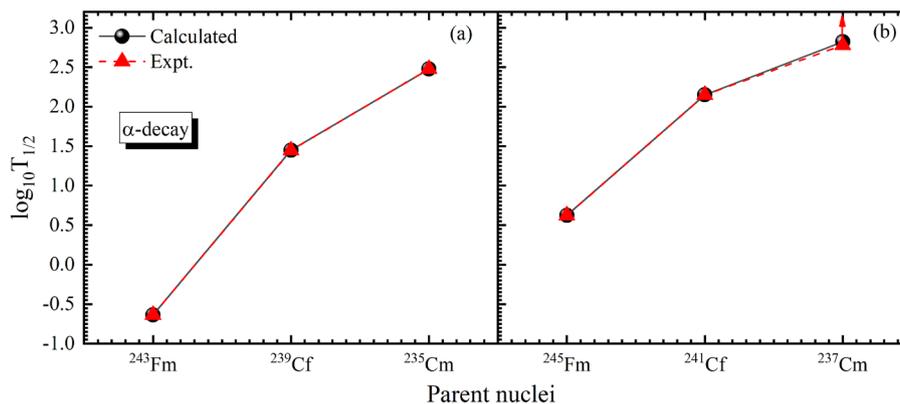

Figure 2: The Logarithmic half-lives for the α–decay of (a)^{243}Fm and (b)^{245}Fm isotopic chains using the R3Y(NL3*) NN interaction. The experimental data is taken form Ref. [26]

4. Summary and Conclusions

The decay and barrier properties such as the neck-length, barrier lowering, driving potential, α-preformation probability, penetration probability, decay constant, and half-life, across the ^{243,245}Fm isotopic chains are examined using the RMF (NL3*) frame work within the preformed cluster-decay model (PCM). In all cases, the calculated half-lives are found to agree with the experimental data. The central role of the Q-value and its relationship with other observables is analyzed. For the first time, we have shown that an enhanced scaling factor is a good signature for shell/sub-shell closures within the preformed cluster-decay model. Following our observation, α-decay could be the most probable decay mode for ^{243}Fm and ^{245}Fm isotopes. However, parameterization may play an important role in the α-decay half-life predictions. This effect would be incorporated in our subsequent investigation.

Acknowledgements

Authorship contribution

All the authors have contributed equally in preparations of this manuscript.

Funding

Declaration

It is an original data and has neither been sent elsewhere nor published anywhere.

References

[1] G. Gamow, Z. Phys. **51**, 204 (1928). https://doi.org/10.1007/BF01343196

[2] U. Condon, R. W. Gurney, Nature **122**, 439 (1928). https://doi.org/10.1038/122439a0.

[3] H. J. Mang, Ann. Rev. Nucl. Sci. **14**, 1 (1964). https://doi.org/10.1146/annurev.ns.14.120164.000245

[4] C. Qi, Rev. Phys. **1**, 77 (2016). https://doi.org/10.1016/j.revip.2016.05.001

[5] H. B. Yang *et al.,* Phys. Lett. B **777**, 212 (2018). https://doi.org/10.1016/j.physletb.2017.12.017

[6] S. Mukherjee, N. L. Singh and J. Rama Rao, Pramana J. Phys. **41**, 311 (1993). https://doi.org/10.1007/BF02847396

[7] H. C. Manjunatha, K. N. Sridhar and N. Sowmya, Phys. Rev. C **98**, 024308 (2018). https://doi.org/10.1103/PhysRevC.98.024308

[8] N. Maroufi, V. Dehghani and S. A. Alavi, Nucl. Phys. A **983**, 77 (2019). https://doi.org/10.1016/j.nuclphysa.2018.12.023

[9] H. C. Manjunatha, G. R. Sridhara, N. Sowmya, P. S. D. Gupta, N. Manjunatha and H. B. Ramalingam, Indian J. Phys. **96**, 2485 (2022). https://doi.org/10.1007/s12648-021-02171-5

[10] W. J. Weber, R. C. Ewing and A. Meldrum, J. Nucl. Mater. **250**, 147 (1997). https://doi.org/10.1016/S0022-3115(97)00271-7

[11] V. Yu. Denisov and H. Ikezoe, Phys. Rev. C **72**, 064613 (2005). https://doi.org/10.1103/PhysRevC.72.064613

[12] Y. He, X. Yu and H. F. Zhang, Chin. Phys. C **45**, 014110 (2005). https//doi.org/10.1088/1674-1137/abc684.

[13] D. Ni. and Z. Ren. Phys. Rev. C **81**, 064318 (2010). https://doi.org/10.1103/PhysRevC.81.064318

[14] D. Ni and Z. Ren, Nucl. Phys. A **893**, 13 (2012). https://doi.org/10.1016/j.nuclphysa.2012.08.006

[15] R. Blendowske, T. Fliessbach and H. Walliser, Nucl. Phys. A **464**, 75 (1987). https://doi.org/10.1016/0375-9474(87)90423-4

[16] S. S. Malikand R. K. Gupta, Phys. Rev. C **39**, 1992 (1989). https://doi.org/10.1103/PhysRevC.39.1992

[17] B. Buck and J. C. Johnston, A. C. Merchant, and S. M. Perez, Phys. Rev. C **53**, 2841 (1996). https://doi.org/10.1103/PhysRevC.53.2841

[18] R. Kumar and M. K. Sharma, Phys. Rev. C **85**, 054612 (2012). https://doi.org/10.1103/PhysRevC.85.054612

[19] R. Kumar, Phys. Rev. C **86**, 044612 (2012). https://doi.org/10.1103/PhysRevC.86.044612

[20] *Nuclear Structure Physics*, edited by A. Shukla and S. K. Patra, (CRC Press, Boca Raton, 2020). ISBN: 9780367256104.

[21] G. R. Satchler and W. G. Love, Phys. Reports **55**, 183 (1979). https://doi.org/10.1016/0370-1573(79)90081-4

[22] M. Bhuyan, R. Kumar, S. Rana, D. Jain, S. K. Patra and B. V. Carlson, Phys. Rev. C **101**, 044603 (2020). https:// doi.org/10.1103/PhysRevC.101.044603

[23] M. Bhuyan and R. Kumar, Phys. Rev. C **98**, 054610 (2020). https:// doi.org/10.1103/PhysRevC.98.054610

[24] B. B. Singh, M. Bhuyan, S. K. Patra, and R. K. Gupta, J. Phys. G: Nucl. Part. Phys. **39**, 025101 (2012). http://dx.doi.org/10.1088/0954-3899/39/6/069501

[25] B. B. Sahu, S. K. Singh, M. Bhuyan, S. K. Biswal, and S. K. Patra, Phys. Rev. C **84**, 034614 (2014). https://doi.org/10.1103/PhysRevC.89.034614.

[26] J. Khuyagbaatar, *et al.*, Phys. Rev. C **102**, 044312 (2020). https://doi.org/10.1103/PhysRevC.102.044312

[27] J. G. Deng, H. F. Zhang, Phys. Rev. C **102**, 044314 (2020). https://doi.org/10.1103/PhysRevC.102.044314.

[28] J. G. Deng, H. F. Zhang, Chin. Phys. C **45**, 024104 (2021). https://doi.org/10.1088/1674-1137/abcc5a

[29] *Relativistic Density Functional for Nuclear Structure*, edited by J. Meng, Int. Rev. Nucl. Phys. (Word Scientific, Singapore, 2016), **10**, https://doi.org/10.1142/9872

[30] G. A. Lalazissis, S. Karatzikos, R. Fossion, D. Pena Arteaga, A. V. Afanasjev and P. Ring, Phys. Lett. B **671**, 36 (2009). https://doi.org/10.1016/j.physletb.2008.11.070

[31] P. Ring, Prog. Part. Nucl. Phys. **37**, 193 (1996). https://doi.org/10.1016/0146-6410(96)00054-3

[32] J. W. Negele and Erich Vogt (PlenumPress, New York, 1986), B. D. Serot and J. D. Walecka, **16**, p. 1; ISBN: 0306419971 9780306419973.

[33] S. S. Malik and R. K. Gupta, Phys. Rev. C **39**, 1992 (1989). https://doi.org/10.1103/PhysRevC.39.1992

[34] J. T. Majekodunmi, M. Bhuyan, D. Jain, K. Anwar, N. Abdullah, and Raj Kumar, Phys. Rev. C **105**, 044617 (2022). https://doi.org/10.1103/PhysRevC.105.044617

[35] J. Blocki, J. Randrup, W. J. Swiatecki, and C. F. Tsang, Ann. Phys. (N.Y.) **105**, 427 (1977). https://doi.org/10.1016/0003-4916(77)90249-4

[36] R. Kumar, K. Sandhu, M. K. Sharma, and R. K. Gupta, Phys. Rev. C **87**, 054610 (2013). https://doi.org/10.1103/PhysRevC.87.054610

[37] Niyti, G. Sawhney, M. K. Sharma, and R. K. Gupta, Phys. Rev. C **91**, 054606 (2015). https://doi.org/10.1103/PhysRevC.91.054606

[38] J. A. Pattnaik, T. M. Joshua, A. Kumar, M. Bhuyan and S. K. (2021). https://doi.org/10.1103/PhysRevC.105.01431

[39] J. A. Pattnaik, M. Bhuyan, R. N. Panda and S. K. Patra, Phys. Scr. **96**, 125319 (2021). https://doi.org/10.1088/1402-4896/ac3a4d

[40] A. Kumar, H. C. Das, M. Kaur, M. Bhuyan, S. K. Patra, Phys. Rev. C **103**, 024305 (2021). https://doi.org/10.1103/PhysRevC.103.024305